Vapor−Liquid and Vapor−Solid Phase Equilibria of Fullerenes: The Role of the Potential Shape on the Triple Point

Bin Chen,*,† J. Ilja Siepmann,‡ Sami Karaborni,§ and Michael L. Klein||

Department of Chemistry, Louisiana State University, Baton Rouge, Louisiana 70803-1804, Departments of Chemistry and of Chemical Engineering and Materials Science, University of Minnesota, 207 Pleasant Street Southeast, Minneapolis, Minnesota 55455-0431, Pharmaceutical Research & Development, Merck & Company Inc., P.O. Box 4, WP78-304, West Point, Pennsylvania 19486, and Center for Molecular Modeling and Department of Chemistry, University of Pennsylvania, 231 South 34th Street, Philadelphia, Pennsylvania 19104-6323

Received: July 18, 2003; In Final Form: August 22, 2003

Gibbs ensemble Monte Carlo simulations were carried out to calculate the vapor−liquid and vapor−solid coexistence curves for three fullerenes: C_{60}, C_{70}, and C_{96}. Single-site potentials with parameters proposed by Girifalco and Pacheco/Ramalho were used to describe the interactions of the fullerene molecules. It is observed that the liquid-phase temperature range (as measured by the reduced triple point temperature, T_t/T_c) decreases considerably for C_{60} compared to 12−6 Lennard-Jonesium and eventually disappears for C_{96} as the potential wells become narrower with increasing molecular weight of the fullerenes. This confirms previous theoretical predictions that the width of the potential well has an important influence on the overall shape of a phase diagram. However, calculations of reduced second virial coefficients show that the fullerene phase diagrams can be described by an extended principle of corresponding states. The Gibbs ensemble simulations yield a triple point temperature of 1876 ± 13 K for C_{60} and the Girifalco potential, in excellent agreement with recent calculations by Hasegawa and Ohno and Costa et al.

Knowledge of phase diagrams is of fundamental importance for the molecular sciences and of practical importance for product and process development in all branches of the chemical industry. The past 15 years have brought advances in molecular simulation algorithms and in transferable force fields that are now enabling the routine calculation of vapor−liquid and liquid−liquid phase equilibria even for relatively complex molecules and multicomponent systems. However, the precise calculation of fluid−solid phase equilibria remains a challenge for molecular simulation and present techniques require thermodynamic integration starting from ideal systems (e.g., the Einstein solid or the ideal gas) for which analytical values of the free energy are available.[1−5] Recently, we proposed an extension of the Gibbs ensemble Monte Carlo (GEMC) method, which allows for the direct calculation of vapor−solid coexistence curves.[6] Here the GEMC method was applied to investigate the complete phase diagrams for medium-sized fullerenes.

Theoretical and computational efforts toward understanding the phase behavior of fullerene systems started immediately after these substances were discovered. However, until now the results remain somewhat inconclusive. About a decade ago, a controversy emerged whether a stable liquid phase exists for C_{60}. Using an integral-equation approach combined with molecular dynamics simulations, Cheng et al.[7] predicted that a liquid phase is present over a very narrow temperature range. In contrast, using GEMC simulations for the vapor−liquid phase equilibria and the Frenkel−Ladd method for the fluid−solid coexistence curve, Hagen et al.[8] reported that the (metastable) critical point is 35 K below the sublimation line. Although it is now generally believed that a very small liquid−vapor phase equilibrium region is present for C_{60},[9] the exact location of this region in the complete phase diagram remains uncertain. For example, over the years many research groups have reported triple point temperatures, T_t, but these are scattered over a disturbingly wide range from 1400 to 1900 K.[10]

Without question the phase behavior of fullerenes differs qualitatively from that of the other spherical molecules, such as argon, methane, or neopentane. Whereas the reduced triple point temperature for these molecules lies close to 0.5, the corresponding value for C_{60} is close to 1. Although the pair interactions for most spherical molecules (or even the individual pair of C atoms on two fullerene molecules) can be described by a Lennard-Jones 12−6 type of potential, the effective intermolecular potential between two fullerene molecules is no longer Lennard-Jones-like. As shown by Girifalco,[11,12] at sufficiently high temperatures when fullerenes can rotate freely, the effective potential between two fullerene molecules can be derived by integrating the interactions between pairs of carbon sites that are uniformly distributed on two cages. The resulting potential is characterized by a harshly repulsive core followed by an attractive well that is much narrower and for which the attractive interactions decay much more rapidly with the intermolecular distance than the usual r^{-6} dependence for dispersive interactions. The functional form of the empirical Girifalco potential (GP) for fullerenes is

$$u(r) = \beta\left[\frac{1}{s(s-1)^9} + \frac{1}{s(s+1)^9} - \frac{2}{s^{10}}\right] - \alpha\left[\frac{1}{s(s-1)^3} + \frac{1}{s(s+1)^3} - \frac{2}{s^4}\right] \quad (1)$$

* Corresponding author: binchen@lsu.edu.
† Louisiana State University.
‡ University of Minnesota.
§ Merck & Company Inc..
|| University of Pennsylvania.

10.1021/jp0361069 CCC: $25.00
Published on Web 10/11/2003

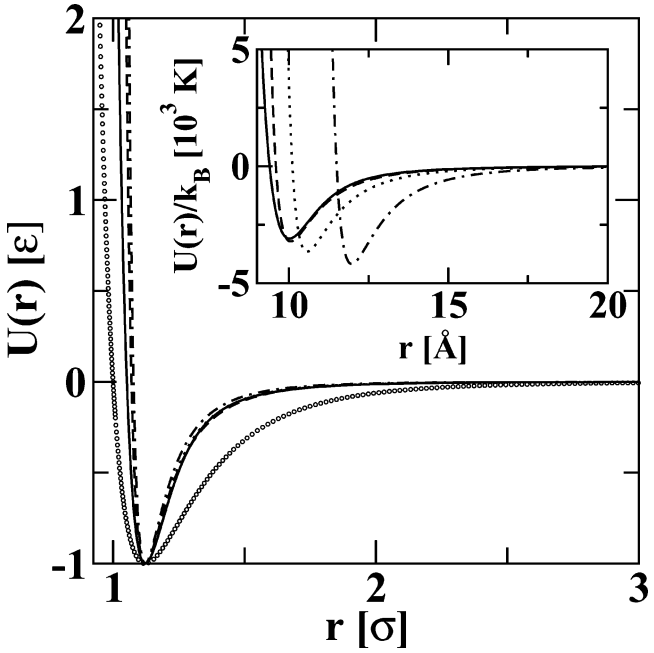

Figure 1. Plot of the 12−6 Lennard-Jones potential (circles) that describes the pair interaction of many simple spherical molecules, the Pacheco/Ramalho potential for C_{60} (solid line), and the Girifalco potentials for C_{60} (dashed line), C_{70} (dotted line), and C_{96} (dashed−dotted line). For direct comparison, the fullerene potentials (shown in the inset) were scaled to yield the same position and depth of the potential energy minimum as the Lennard-Jones potential. Note that the intermolecular interaction for fullerene systems is very short-ranged and the attractive well becomes narrower with increasing carbon number.

with $s = r/2a$ and the α and β parameters given in the original articles.[12] A second single-site potential for C_{60} was proposed by Pacheco and Ramalho (PRP)[13] using electronic structure methods and is given by

$$u(r) = \left[1 + \exp\left(\frac{r-\mu}{\delta}\right)\right]^{-1} M_0 \exp\left[\tau\left(1 - \frac{r}{d_0}\right)\right] \times \left\{\exp\left[\tau\left(1 - \frac{r}{d_0}\right)\right] - 2\right\} + \left\{1 - \left[1 + \exp\left(\frac{r-\mu}{\delta}\right)\right]^{-1}\right\} \times \left(-\frac{C_6}{r^6} - \frac{C_8}{r^8} - \frac{C_{10}}{r^{10}} - \frac{C_{12}}{r_{12}}\right) \quad (2)$$

with parameters defined in the original article. A comparison between the Lennard-Jones 12−6 potential and pair potentials for some fullerenes is shown in Figure 1.

In this work, the Gibbs ensemble Monte Carlo (GEMC) method was used for the calculation of both liquid−vapor and solid−vapor phase coexistence curves. As in the original GEMC method,[14,15] two simulation boxes are employed to simulate the two thermodynamically connected phases. These two boxes are physically separated but are in thermodynamic contact through volume and particle exchanges. For solid−fluid phase equilibria, however, insertions and removals of single particles are extremely inefficient because they involve the creation of interstitial or vacancy defects in the crystalline phase. This problem can be overcome by a simple extension of the GEMC approach proposed recently by us.[6] For solid−vapor phase equilibria, the box that contains the solid phase is elongated along one axis and contains only a slab of solid material surrounded on both sides by vapor regions, thereby allowing for efficient particle exchanges on the two surfaces. The direct

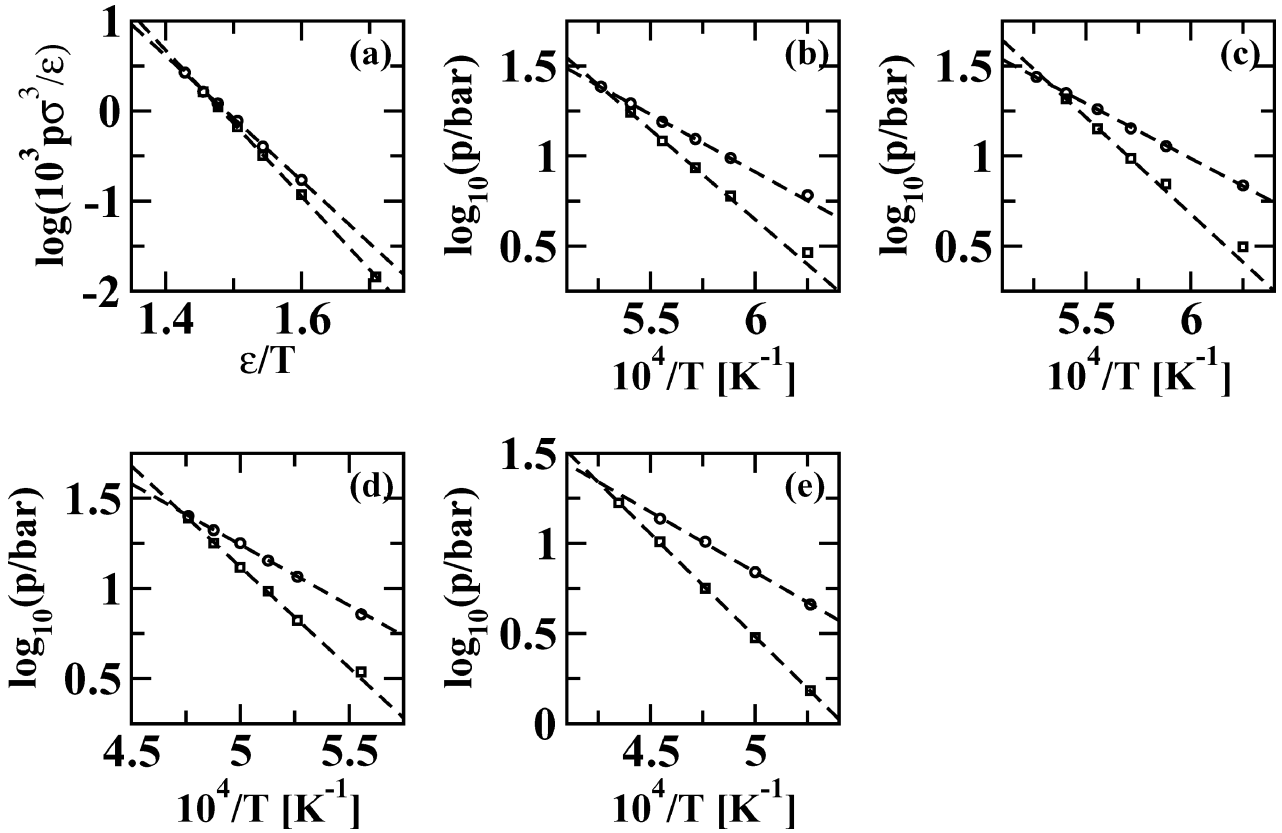

Figure 2. Clausius−Clapeyron plots of the sublimation and vaporization pressure curves for (a) Lennard-Jonesium, (b) C_{60} (PRP), (c) C_{60} (GP), (d) C_{70}, and (e) C_{96} vs the inverse temperature. The squares and circles represent the data from Gibbs ensemble simulations using the solid-slab or the conventional setup, respectively. Statistical errors in the pressure are smaller than the symbol size. The dashed lines depict weighted-linear least-squares fits to the sublimation and vapor pressure data obtained from the Gibbs ensemble simulations.

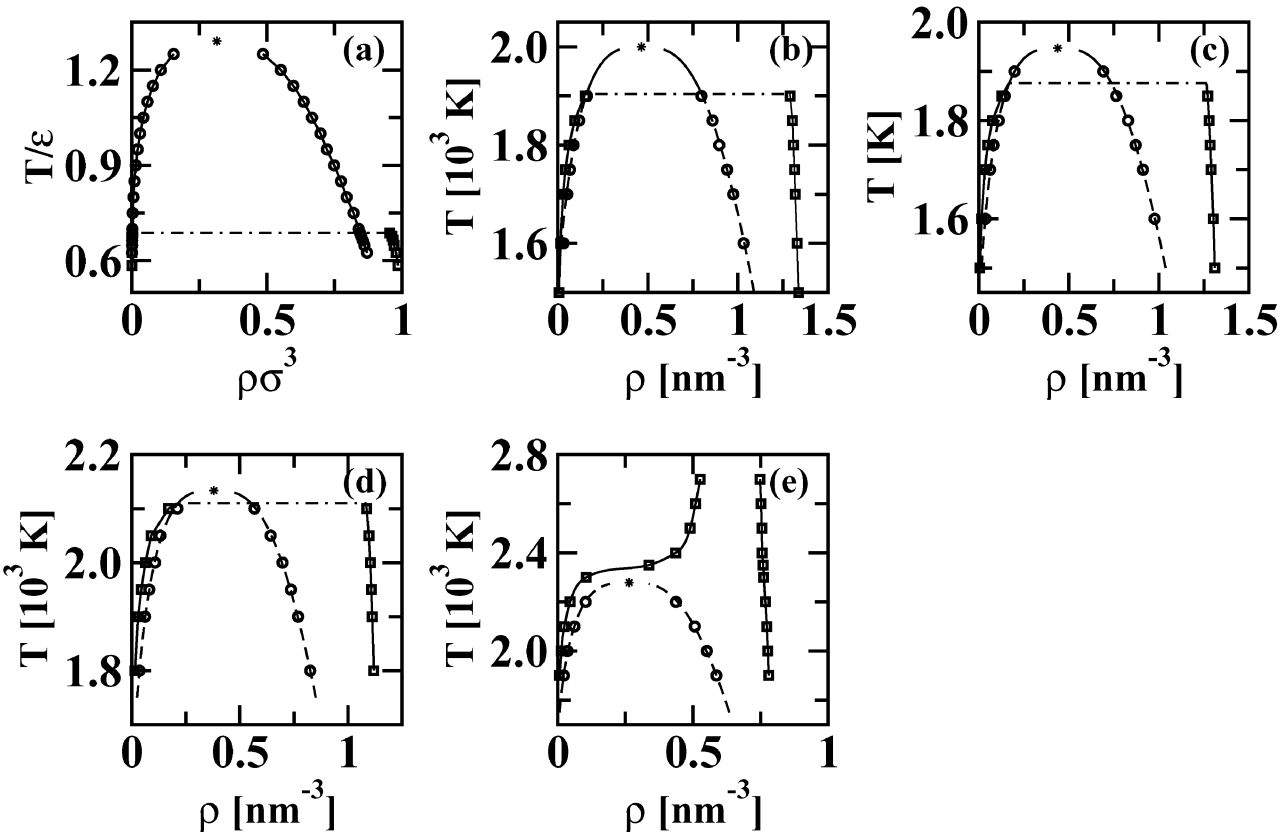

Figure 3. Temperature−number density phase diagrams for (a) Lennard-Jonesium, (b) C_{60} (PRP), (c) C_{60} (GP), (d) C_{70}, and (e) C_{96}. Squares and circles as in Figure 2. The stars are the estimates of the critical points. The solid lines are the guide for the eye showing the stable phase coexistence curves. The dashed−dotted lines depict the triple point temperature, which is missing for C_{96}. The dashed lines are fits of the vapor−liquid coexistence curves to the scaling law.[15]

GEMC approach has been shown to yield results for Lennard-Jonesium[6] that are in excellent agreement with the simulations using the Gibbs−Duhem integration technique.[5]

The GEMC simulations were carried out for relatively large system sizes: 1728 and 1000 particles for the vapor−solid and vapor−liquid coexistence curves, respectively. For all simulations, a spherical potential truncation at a value close to 4σ was used. Due to the inhomogeneous nature of the solid-slab box, tail corrections were not used for any of the simulations (but given the short-ranged nature of the fullerene potentials and the relatively large cutoff values used here, it is expected that tail corrections would not alter the results significantly). The configurational-bias algorithm[16] with multiple choices for the insertion/removal location was used to improve the acceptance rate of the particle swap moves. The production periods consisted of more than 400 000 Monte Carlo cycles (where each Monte Carlo cycle involves N moves). For the 1000-particle systems, a simulation run of this length took about 1 day on a Pentium IV 2.4 GHz machine. The triple point and critical temperatures were estimated directly from the intersection of Clausius−Clapeyron plots and using fits to the scaling law, respectively. The use of the scaling law and the finite size (number of particles) of the simulated system lead to small, but systematic uncertainties for the estimation of the critical temperature. For the Lennard-Jonesium system, GEMC simulations yielded an estimate of $T_c^* = 1.304 \pm 0.005$,[17] whereas the accepted value from GCMC simulations with mixed-field finite-size scaling reported by Potoff and Panagiotopoulos is 1.3120 ± 0.0007.[18]

Figure 2 shows the pressure−(inverse) temperature phase diagrams for Lennard-Jonesium, C_{60}, C_{70}, and C_{96}. For all cases, both the sublimation and vaporization pressure lines can be fit well by straight lines, as prescribed by the Clausius−Clapeyron equation, and the triple point can be located by the intersection of these two lines. The triple point temperatures determined from our simulations are 1876 ± 13, 1904 ± 15, 2110 ± 11, and 2359 ± 18 K, for C_{60} (GP), C_{60} (PRP), C_{70}, and C_{96}, respectively. The corresponding critical temperatures are 1946 ± 4, 2000 ± 7, 2131 ± 4, and 2272 ± 8 K, respectively. For C_{60} and the Girifalco potential, our predicted values are in excellent agreement with recently reported predictions of $T_t = 1875$ K and $T_c = 1940$ K by Costa et al.[9] (using extensive Monte Carlo simulations with a combination of the Widom test particle, Einstein−Ladd, and thermodynamic integration methods) and of $T_t = 1880$ K and $T_c = 1980$ K by Hasegawa and Ohno[19] (using a series of Monte Carlo simulations in the canonical ensemble and a full free energy analysis).

In contrast, Fartaria et al.[10] obtained a significantly lower value for the triple-point temperature, $T_t = 1529 \pm 36$ K, whereas their estimate for the critical temperature, $T_c = 1951 \pm 28$ K agrees well with our estimate, albeit one should note the difference in the statistical uncertainties. In their calculations, the triple point was determined using the original GEMC approach. Specifically, the temperature employed for the GEMC vapor−liquid phase equilibrium calculations is gradually decreased until a temperature is reached below which the liquid phase is no longer stable, and this temperature was used to estimate the triple point. Considering that spontaneous freezing usually happens only for deeply supercooled systems,[20] this method is very likely to underestimate in a systematical way the triple point temperature. Indeed, the triple point temperature of 1694 ± 49 K for C_{70} reported by Silva Fernandes et al.[21] is again much lower than our estimate. However, again their estimate of $T_c = 2131 \pm 44$ agrees well with our GEMC data.

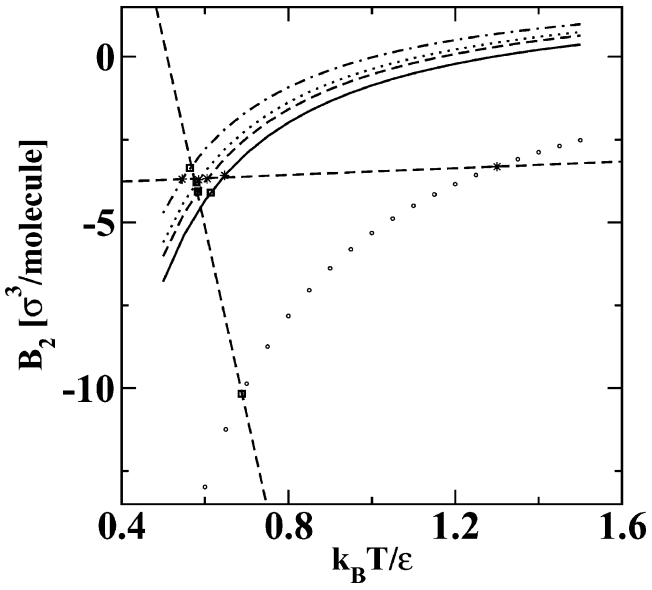

Figure 4. Plot of the temperature dependence of the reduced second virial coefficients for Lennard-Jonesium, C_{60} (PRP), C_{60} (GP), C_{70}, and C_{96}. For fullerene systems, these values were obtained using the scaled potentials ($r_{min} = 2^{1/6}\sigma$ and $U(r_{min}) = -\epsilon$) shown in the main part of Figure 1. Line styles as Figure 1. Stars and squares denote the B_2^* values at the critical and triple points, respectively. Note that these values fall on two straight lines, one nearly horizontal and the other with large negative slope.

Silva Fernandez and co-workers[10,21] have repeatedly argued that "high-temperature results (for the triple points) correspond to local minima of the Gibbs free energy, whereas the low-temperature results correspond to the global minima of the free energy." However, the Clausius−Clapeyron plots shown in Figure 2 demonstrate unambiguously that the saturated vaporization pressures are higher than the saturated sublimation pressures below the "high-temperature" triple points. Because the chemical potential of the vapor phase increases with pressure,[22] it is obvious that the phase with the lower saturation pressure also has the lower Gibbs free energy.

For C_{96}, the triple point temperature of 2359 K extrapolated from the Clausius−Clapeyron plot is, in fact, above the liquid−vapor critical point (2272 K). As can be seen from the representation of the phase diagram in the temperature−density plane (shown in Figure 3), the sublimation line passes about 55 K above the liquid−vapor critical point. Because all phases that occur below the sublimation line have a higher Gibbs free energy than the coexisting solid and vapor phases, C_{96} is actually one of those systems for which a stable liquid phase does not exist. In comparison, both C_{60} and C_{70} possess relatively small vapor−liquid phase equilibrium regions, much smaller than that of 12−6 Lennard-Jonesium or carbon dioxide, which has the smallest liquid-phase range of common organic molecules.[6]

Recently, Noro and Frenkel[23] proposed an extension of the principle of corresponding states to systems with different ranges of the attractive interactions. To test whether the critical and triple point temperatures calculated in this work follow a principle of corresponding states, we calculated the (reduced) second virial coefficients, B_2^*, for the scaled potentials shown in Figure 1. As was also found by Noro and Frenkel (using a different reduced scale, see Figure 1 of ref 23) and Vliegenhart and Lekkerkerker,[24] the values of B_2^* at the critical temperature fall onto a horizontal line (see Figure 4); i.e., they are nearly constant. In addition, the values of B_2^* at the triple point temperature fall onto a different line with large negative slope that intersects the critical-point line at $T^* = 0.57$, thereby, confirming that there is a distinct threshold value below which a stable liquid phase does not exist.[23]

In conclusion, using conventional GEMC simulations for vapor−liquid phase equilibria and solid-slab GEMC simulations for vapor−solid phase equilibria, the critical and triple points of three fullerenes were evaluated. These simulations demonstrate that for C_{60} a liquid phase is thermodynamically stable over a small range of only 70 K. The stable liquid range is found to diminish further for C_{70} and to vanish for C_{96}. Thus, the relative narrowness of the interaction potential (i.e., the short range of the attractive part for square-well potentials) controls whether a liquid phase is stable. These results support an extended law of corresponding states for systems with different ranges of the attractive interactions, such as colloids, proteins, and many other nanoparticles. Below a certain threshold value, there is no stable vapor−liquid transition and the system will directly condense to a crystalline phase.

Acknowledgment. Financial support from the National Science Foundation CTS-0138393 (J.I.S.) and CHE-0205146 (M.L.K.) is gratefully acknowledged. Part of the computer resources were provided by the Minnesota Supercomputing Institute.

References and Notes

(1) Frenkel, D.; McTague, J. P. *Annu. Rev. Phys. Chem.* **1980**, *31*, 491.
(2) Frenkel, D.; Ladd, A. J. C. *J. Chem. Phys.* **1984**, *81*, 3188.
(3) Kuchta, B.; Etters, R. D. *Phys. Rev. B* **1993**, *47*, 14691.
(4) Malanoski, A. P.; Monson, P. A. *J. Chem. Phys.* **1999**, *110*, 664.
(5) Kofke, D. A. *J. Chem. Phys.* **1993**, *98*, 4149.
(6) Chen, B.; Siepmann, J. I.; Klein, M. L. *J. Phys. Chem. B* **2001**, *105*, 9840.
(7) Cheng, A.; Klein, M. L.; Caccamo, C. *Phys. Rev. Lett.* **1993**, *71*, 1200.
(8) Hagen, M. H. J.; Meijer, E. J.; Mooij, G. C. A. M.; Frenkel, D.; Lekkerkerker, H. N. W. *Nature* **1993**, *365*, 425.
(9) Costa, D.; Pellicane, G.; Abramo, M. C.; Caccamo, C. *J. Chem. Phys.* **2003**, *118*, 304.
(10) Fartaria, R. P. S.; Fernandes, F. M. S. S.; Freitas, F. F. M. *J. Phys. Chem. B* **2002**, *106*, 10227.
(11) Girifalco, L. A. *J. Phys. Chem.* **1991**, *95*, 5370.
(12) Girifalco, L. A. *J. Phys. Chem.* **1992**, *96*, 858.
(13) Pacheco, J. M.; Ramalho, J. P. P. *Phys. Rev. Lett.* **1997**, *79*, 3873.
(14) Panagiotopoulos, A. Z.; Quirke, N.; Stapleton, M.; Tildesley, D. J. *Mol. Phys.* **1988**, *63*, 527.
(15) Smit, B.; de Smedt, P.; Frenkel, D. *Mol. Phys.* **1989**, *68*, 931.
(16) Siepmann, J. I.; Frenkel, D. *Mol. Phys.* **1992**, *75*, 59.
(17) Simulations were carried out for 1000 particles with a spherical potential truncation at 4σ and appropriate tail corrections. Only the phase coexistence densities obtained at $T^* = 1.15$ or higher were used in the fits to the scaling law (with a scaling exponent of $\beta = 0.325$) for the estimation of the critical temperature.
(18) Potoff, J. J.; Panagiotopoulos, A. Z. *J. Chem. Phys.* **1998**, *109*, 10914.
(19) Hasegawa, M.; Ohno, K. *J. Chem. Phys.* **1999**, 111, 5955.
(20) ten Wolde P. R.; Ruiz-Montero, M. J.; Frenkel, D. *J. Chem. Phys.* **1996**, *104*, 9932.
(21) Silva Fernandes, F. M. S.; Freitas, F. F. M.; Fartaria, R. P. S. *J. Phys. Chem. B* **2003**, *107*, 276.
(22) Castellan, G. W. *Physical Chemistry*, 3rd ed.; Benjamin/Cummings Publishing: Menlo Park, CA, 1983.
(23) Noro, M. G.; Frenkel, D. *J. Chem. Phys.* **2000**, *113*, 2941.
(24) Vliegenthart, G. A.; Lekkerkerker, H. N. W. *J. Chem. Phys.* **2000**, *112*, 5364.